Journal of Applied Pharmaceutical Science Vol. 10(08), pp 095-104, August, 2020
Available online at http://www.japsonline.com
DOI: 10.7324/JAPS.2020.10811
ISSN 2231-3354

# Formulation and optimization of Enalapril Maleate-loaded floating microsphere using Box–Behnken design: *in vitro* study

Vijay Bahadur Kumal, Chhitij Thapa*, Prakash Ghimire, Pradyumna Chaudhari, Jitendra Yadhav
Department of Pharmacy, Universal College of Medical Sciences, Tribhuwan University, Siddhartha Nagar, Nepal.

**ARTICLE INFO**

Received on: 27/12/2019
Accepted on: 21/06/2020
Available online: 05/08/2020

***Key words:***
Enalapril Maleate, floating microsphere, Box–Behnken design, controlled release, solvent evaporation.

**ABSTRACT**

The objective was to prepare an Enalapril Maleate (EnM)-loaded floating microsphere with minimum particle size, maximum drug loading, and drug entrapment efficiency. Formulations were prepared by varying drug-to-polymer ratio (A), solvent ratio (B), and stirring time (C). The solvent evaporation method was used to prepare the microsphere. "Box–Behnken's design" (3 factors × 3 levels) was utilized for optimization. The independent variables were polymer-to-drug ratio (A), solvent ratio (B), and stirring time (C), while particle size ($R^1$), drug loading ($R^2$), and entrapment efficiency ($R^3$) were considered as dependent variables. EnM-loaded alcohol microsphere (Formulation-A) was prepared and optimized. Both Formulation-A and EnM-loaded acetonitrile microspheres (Formulation-B) were subjected to morphological, micrometric, characterization, and *in vitro* release studies. The particle size, drug loading, and entrapment efficiency of Formulation-A and Formulation-B were 143 ± 27.75 µm, 37.31% ± 5.73%, and 76.89% ± 4.97%, and 158.13 ± 25.1 µm, 40.13% ± 6.12%, and 99.19% ± 1.14%, respectively. The cumulative drug releases of Formulation-A and Formulation-B were 90.52% ± 4.11% and 86.23% ± 3.81%, respectively. Both formulations followed the Higuchi model of drug release. EnM-floating microsphere was effectively prepared and both formulations showed excellent continuous release properties for more than 12 hours.

## INTRODUCTION

Because of its high frequency and concomitant hazards of cardiovascular and kidney diseases, hypertension (HTN) is a major public health challenge globally. It was recognized as the leading mortality risk factor (Campbell *et al*., 2012). The incidence of HTN has been commonly recorded in different areas of the globe and the issues connected with HTN are rising more quickly in developing countries, such as Nepal. The study revealed that the prevalence of HTN in Nepal's rural society and the urban area has increased threefold (Vaidya *et al*., 2012). The oral route is extensively utilized to deliver the therapeutic agents for the management of HTN due to the low treatment price and ease of administration, resulting in elevated patient compliance rates. Over 50% of the market's drug delivery systems are oral drug delivery systems (Asija *et al*., 2015). The conventional drug delivery system achieves and holds the drug concentration within the optimum therapeutic range necessary for therapy, only if administered multiple times a day (Wen *et al*., 2015). This results in significant fluctuation in drug levels. Hence, to overcome these issues, several technical advancements have been made, such as novel drug delivery systems (NDDS) that can significantly improve the medication method and deliver several therapeutic advantages (Gao and Jiang, 2017). Despite the benefits of NDDS in terms of therapeutic considerations, there are several technical and biological challenges. For instance, modifying the GI transit time is a promising challenge for the formulation of an oral controlled drug delivery system (Ammar *et al*., 2016). Conventional drug delivery systems like tablets and capsules offer a particular concentration of drugs in the systemic circulation, lacking control over the rate of drug delivery, as well as triggering significant changes in the concentrations of plasma drugs. Moreover, there is a considerable fluctuation in the gastric emptying rate. Less time spent in the gut may result in inadequate drug absorption. Besides, the magnitude of absorption in the stomach or upper intestine is

*Corresponding Author
*Chhitij Thapa, Department of Pharmacy, Universal College of Medical Sciences, Tribhuwan University, Siddhartha Nagar, Nepal.*
*E-mail: kshitizthapa07 @ gmail.com*

higher (Zhang *et al*., 2016). Hence, to figure the limitation of the single oral dosage form, the concept of a floating controlled drug delivery system was taken into account. Several types of control drug delivery systems have been discovered, out of which the concept of floating microencapsulation dosage form was found to be convincing in terms of its financial and technical prospects. Moreover, it was found to be more effective in addressing the several issues of conventional dosage form, especially concerning their therapeutic and safety issues (Bhardwaj *et al*., 2014; Farooq *et al*., 2017).

Microencapsulation is defined as "… a method by which solid, fluid, or gaseous active ingredients are packaged in a second product to protect the active ingredient from the surroundings." (Hu *et al*., 2017) Microencapsulation is primarily known to convert the liquids into solids, by altering the surface and colloidal properties, offering a barrier for environmental protection and regulating the rate of release or availability features of coated materials. Macropackaging techniques can achieve several of these properties; however, the uniqueness of microencapsulation is the size and successive uses of the covered particles (Chatterjee *et al*., 2014). The study is based on the management of HTN with Enalapril Maleate (angiotensin-converting enzyme inhibitor) as a drug of choice that is 60% absorbed and undergoes de-esterification converting into an active metabolite enalaprilat, a potential angiotensin-converting enzyme inhibitor (Thabet *et al*., 2018). It is efficient against essential and reno-vascular HTN and cardiac congestion (Ipate *et al*., 2018; Swamy *et al*., 2013). Enalapril Maleate (EnM) microsphere increases bioavailability and compliance by decreasing the frequency of administration and helps maintain the consistency of plasma drug concentration during drug therapy (Ammar *et al*., 2016; Nila *et al*., 2014).

## MATERIALS AND METHODS

EnM (an active pharmaceutical ingredient) was kindly gifted by Lomus Pharmaceutical, Nepal. Hydroxyl propyl methylcellulose (HPMC) was purchased from Kemphasol. Calcium chloride was purchased from Quligen Fine Chemicals. Dichloromethane (DCM) was purchased from Avantor Performance Ltd. Ethylcellulose (EC) and sodium alginate (Na-Alg) polymer, Tween 80, and other solvents such as ethyl alcohol and acetonitrile (ACN) were purchased from S.D. Fine Limited. All of the materials and solvents were of analytical grade.

### Formulation of floating microsphere

The formulation of the EnM-loaded alcohol microsphere (Formulation-A) was carried out by a solvent evaporation method (Prajapati *et al*., 2012). Weighed quantity of EnM (5 mg) and a suitable amount of polymers (EC and HPMC) of varying proportions were dissolved in a mixture of varying proportions of DCM and ethanol. The resulting solution was dropwise introduced into the distilled water containing 0.6% Tween 80 as a surfactant. The entire solution was stirred at the agitation speed of 1,200 rpm for 45 minutes. After the complete evaporation of the volatile solvent, the emulsion was filtered and washed with distilled water (2–3 washes). The collected microspheres were air-dried and stored in desiccators. Similarly, another EnM-loaded ACN microsphere (Formulation-B) was formulated by using varying proportions of DCM and ACN as a solvent medium. The solubility of EnM was higher in ethanol and sparingly soluble in DCM and ACN. On the higher temperature, HPMC was soluble in water, while insoluble in DCM and ACN. EC was insoluble in water, sparingly soluble in DCM and ACN, but freely soluble in ethanol. The selection of the solvent medium was based on the earlier studies that confirm the use of solvents like DCM and ACN in various food and pharmaceutical industries (Amid *et al*., 2015). A comparison of Formulation-B was made with Formulation-A.

### Optimization of formulation

The optimization of the EnM-loaded microsphere was carried out by using design expert 10 (State-Ease Inc., Minneapolis, MN). Three independent variables, that is, polymer-to-EnM ratio (A), alcohol-to-DCM ratio (B), and stirring time (C), were taken into account, and the effect of these independent variables was studied on the observed responses, that is, particle size, drug loading, and entrapment efficiency. The polymer-to-drug ratio used was in the ranges of 50:1, 100:1, and 150:1; similarly, the solvent ratio (DCM: ethanol) was in the ranges of 1:1, 2:1, and 3:1, and stirring time ranged between 20, 40, and 60 minutes. The optimization design is depicted in Table 1. With the 3 factors × 3 levels, 17 different runs were carried out and the response was observed for each run. The best optimized formulation was considered for further study.

## CHARACTERIZATION

### Particle size analysis

Optical microscopy was used for the determination of the particle size of the formulated microspheres. Optical microscope Olympus BX53 was used. Each batch containing more than 300 floating microspheres was placed on a clean slide, and the diameter of the particles was measured randomly. The eyepiece micrometer was calibrated with the help of a stage micrometer. Edmondson's equation was used for the determination of the average particle size (Abbas *et al*., 2014):

$$D_{\text{mean}} = \Sigma_{nd}/\Sigma_{n}$$

where $n$ = number of microsphere checked and $d$ = mean size range.

### Percentage yield

The percentage yield was estimated as the amount of microspheres obtained from the total amount of drugs and

**Table 1.** Optimization design including independent and dependent variables with their responses.

| Independent variable | Level | | |
|---|---|---|---|
| EnM polymer ratio | −1 | 0 | +1 |
| Solvent ratio | −1 | 0 | +1 |
| Stirring time | −1 | 0 | +1 |
| Dependent variable | | Desired response | |
| Particle size | | Minimum | |
| EnM loading % | | Maximum | |
| EnM entrapment efficiency % | | Maximum | |

nonvolatile excipients deployed for the formulation of the microspheres (Gaur *et al*., 2014):

% Yield = (Actual weight of microsphere/Total weight of EnM and polymer) × 100%

**Drug loading and encapsulation efficiency**

Accurately weighed microspheres (100 mg) were kept overnight in 0.1 N HCl for the extraction of the drug. Filtrates were diluted suitably and EnM was quantified spectrophotometrically using UV–Vis spectrophotometer at 207 nm. The percentage of drug loading was calculated as:

$$L = (Q_m/W_m) \times 100\%$$

where $L$ is the percentage drug loading of microspheres, $Q_m$ and $W_m$ represent the quantity of drug and microsphere in gram, respectively (Farooq *et al*., 2017). The percentage of encapsulation was estimated as:

$$E = (Q_p/Q_t) \times 100\%$$

where $E$ is the percentage encapsulation of microspheres, $Q_p$ and $Q_t$ represent the quantity of the drug encapsulated in microspheres and the theoretical drug content in gram, respectively (Garg *et al*., 2010; Senthikumar *et al*., 2010; Sharma *et al*., 2015).

**Micrometric studies of microsphere**

*Bulk density*

To determine the bulk density, suitably weighed microspheres were introduced into the measuring cylinder (100 ml) and the volume was observed, representing bulk quantity that involves real powder quantity and microspheres void space. Bulk density was estimated as the mass of microspheres divided by the volume of microspheres before tapping (Ramteke *et al*., 2015):

Bulk density = (mass of microsphere) / (bulk volume of microsphere)

*Tapped density*

A suitable quantity of the microsphere was introduced into a measuring cylinder and was allowed to tap 100 times using the bulk density apparatus. The final tapped volume of the microsphere was recorded. The tapped density was estimated as the total mass of microspheres divided by the tapped volume of microsphere (Bhardwaj *et al*., 2014):

Tapped density = (mass of microsphere) / (tapped volume of microsphere)

*Carr's (compressibility) index*

Carr's index value of microspheres was estimated as:

% Compressibility = [(tapped density − bulk density) / tapped density] ×100%

For the powders with good flow characteristics, Carr's index value usually lies below 15%, whereas Carr's index above 25% indicates the poor flowability (Farooq *et al*., 2017).

*Hausner's ratio*

Hausner's ratio of microspheres was determined as the ratio of tapped density to the bulk density using the following equation (Agrawal *et al*., 2017; Beringhs *et al*., 2018):

Hausner's ratio = tapped density / bulk density

*Angle of repose*

For the measurement of the resistance of the particle flow, the angle of repose (α) was estimated. The fixed funnel method was used for the determination of the angle of repose. The height of the funnel was adjusted accurately so that there was a narrow space between the tip of the funnel and the heap of the microsphere. Weighed microspheres were passed freely through the funnel on to the surface (Wang *et al*., 2010).

The height and radius of the powder were estimated, and the angle of repose was calculated as (Subham *et al*., 2010):

$\alpha$ = tan-1 h/r

where α = angle of repose,
$h$ = height, and
$r$ = radius of a heap of microsphere

*Test for buoyancy*

The test for the buoyancy of the microspheres was studied in a USP type II dissolution test apparatus. A suitable amount of microspheres (100 mg) was dispersed in the 0.1 M HCl (300 ml) solution. Tween 80 (0.02%) as a surfactant was added to the solution. The medium was stirred with a paddle rotating at 100 rpm, and the temperature was adjusted at 37°C ± 0.5°C. After 12 hours, both the floating and the settled fractions of microspheres were amassed separately by filtration and were dried at 45°C until a constant weight was obtained (Patela *et al*., 2011):

Buoyancy % = [(dried mass of floating microsphere) / (total mass of the microsphere)] ×100%

***In vitro* drug release study**

*In vitro* drug release studies were conducted in a USP type II dissolution apparatus. Accurately weighed floating microspheres (equivalent to 5 mg EnM) were filled into a capsule and introduced in a 900 ml dissolution medium comprising 0.1 N HCL. Tween 80 (0.02%) was added as a surfactant, which helps the solubilization of drugs in the dissolution medium. The medium was stirred with a paddle rotating at the speed of 100 rpm. Samples of 5 ml were withdrawn at 30 minutes, 1, 2, 4, 6, and up to 12 hours. The samples were analyzed by a UV spectrophotometer at 207 nm for the determination of the concentration of drugs present. 5 ml of fresh dissolution medium was introduced after each sampling to maintain the sink condition (Gupta *et al*., 2014; Tamizharasi *et al*., 2011). A similar dissolution study was carried out for the pure drug (5 mg) as well, which worked as a control. The comparative dissolution study was performed for Formulation-A and Formulation-B concerning control.

## RELEASE KINETICS

For the determination of the release kinetics, the data obtained from the *in vitro* drug release study was fitted with various kinetics models (zero-order, first-order, Higuchi, Korsmeyer–Peppas) to understand the general mechanism of drug release from the microsphere. The coefficient of correlation values ($R^2$) was evaluated for each release kinetic model and comparisons were made in between.

## STATISTICAL ANALYSIS

The results of all the experiments were expressed as mean ± SD and were run in triplicate. GraphPad Prism version 7 software (Graph Pad Software Inc., La Jolla, CA) was used to carry out the statistical analysis. A two-way analysis of variance with Tukey's *post-hoc* test was used to analyze the data. Statistical significance was predefined at $p < 0.05$.

## RESULTS AND DISCUSSION

### Statistical optimization by response surface methodology

For the optimization of the formulation, a "Box–Behnken experimental design" was considered using three independent variables at three different levels. The direct influence of the selected independent variables like drug-to-polymer ratio (A), solvent ratio (B), and stirring time (C) on dependent variables like particle size ($R^1$), % drug loading ($R^2$), and % entrapment efficiency ($R^3$) were observed and the observed responses for 17 generated runs are depicted in Table 2.

The best fit model that was chosen for all the three dependent variables, generated by the design expert software 10 (State-Ease Inc., Minneapolis, MN), was the quadratic model with a coefficient of correlation ($R^2$) close to 1. The summary of the model of regression analysis for responses $R^1$, $R^2$, and $R^3$ and regression equation for a fitted quadratic model is depicted in Table 3.

### Response 1 ($R^1$): effect of independent variables on particle size

The $R^2$ of the particle size was 0.9952; the adjusted $R^2$ was 0.9890, and the predicted $R^2$ was 0.9677, representing a reasonable agreement; that is, the difference is less than 0.2.

The Model F-value of 160.96 indicates that the model is significant ($p < 0.05$). In this case, A, C, AC, and $C^2$ are significant model terms.

The 3D response surface plot unveiling the influence of the independent variables on the particle size is shown in Figure 1. This study unveils the fact that with the increase in the polymer-to-drug ratio (A), the particle size of the Formulation-A was increased. This may be due to a greater concentration of the polymer in the formulation solution which may require greater force to breakdown the polymer into finer particles (Jagtap *et al*., 2012). On the contrary, the size of the microsphere was decreased with the increase in solvent ratio (B) (DCM: alcohol). When a good drug solubilizing solvent (alcohol) diffuses into the poor drug solubilizing solvent (DCM), it causes the precipitation of the EnM and the polymer; hence less DCM volume results in greater precipitation resulting in greater particle size (Savjani *et al*., 2012).

**Table 3.** Summary of the results of regression analysis for responses $R^1$, $R^2$, and $R^3$ fitting the quadratic models.

| Quadratic model | $R^2$ | Adjusted $R^2$ | Predicted $R^2$ |
|---|---|---|---|
| Particle size ($R^1$) | 0.9952 | 0.9890 | 0.9677 |
| EnM loading ($R^2$) | 0.7846 | 0.5076 | −1.9034 |
| Entrapment efficiency ($R^3$) | 0.8297 | 0.6108 | −5.5631 |

Regression equation for the fitted quadratic model.

Particle size = +149.30+15.27×A-3.61×B-97.28×C+5.21×AB-10.17×AC+6.46×BC+0.7070×$A^2$+0.0070×$B^2$+39.42×$C^2$.

EnM loading = +35+5.59×A-0.8087×B-0.5288×C+2.24×AB-0.5575×AC+0.52×BC-1.74×$A^2$+0.6075×$B^2$-1.96×$C^2$.

Entrapment efficiency = +79.19+3.70×A+0.4363×B-8.06×C-1.74×AB-0.4575×AC+0.3875×BC-2.18×$A^2$-3.08×$B^2$-1.38×$C^2$.

**Table 2.** Box–Behnken experimental design of Formulation-A and evaluated response parameters ($n = 3$).

| Exp. run | Polymer-EnM ratio (A) | Solvent ratio (B) | Stirring time (C ) | Particle size (µm) | EnM loading % | Entrapment efficiency % |
|---|---|---|---|---|---|---|
| 1 | 50 | 2 | 20 | 260.2 ± 10.57 | 27 ± 4.24 | 77.22 ± 3.21 |
| 2 | 150 | 2 | 20 | 315.21 ± 13.43 | 42 ± 7.31 | 91.17 ± 3.17 |
| 3 | 50 | 3 | 40 | 131.61 ± 17.21 | 25.76 ± 5.67 | 74 ± 2.98 |
| 4 | 150 | 1 | 40 | 158 ± 25.71 | 38 ± 3.25 | 77.34 ± 4.16 |
| 5 | 50 | 1 | 40 | 142 ± 17.56 | 34.01 ± 4.10 | 72.11 ± 3.69 |
| 6 | 100 | 3 | 60 | 91.67 ± 11.21 | 36.57 ± 3.47 | 69.23 ± 2.73 |
| 7 | 50 | 2 | 60 | 84 ± 19.97 | 22.23 ± 4.17 | 61 ± 1.89 |
| 8 | 150 | 2 | 60 | 98.31 ± 16.75 | 35 ± 7.87 | 73.12 ± 5.21 |
| 9 | 100 | 2 | 40 | 143.11 ± 27.75 | 37.31 ± 5.73 | 76.89 ± 4.97 |
| 10 | 100 | 1 | 60 | 93.2 ± 9.35 | 35 ± 6.89 | 65.12 ± 3.91 |
| 11 | 100 | 2 | 40 | 153 ± 10.83 | 33 ± 4.57 | 79.43 ± 2.76 |
| 12 | 100 | 2 | 40 | 141 ± 23.56 | 36.63 ± 6.42 | 75 ± 4.31 |
| 13 | 150 | 3 | 40 | 168.43 ± 13.32 | 38.72 ± 4.51 | 72.27 ± 4.97 |
| 14 | 100 | 2 | 40 | 161.21 ± 18.21 | 33.43 ± 7.25 | 78.03 ± 3.54 |
| 15 | 100 | 3 | 20 | 271.34 ± 31.71 | 31.76 ± 8.10 | 83.56 ± 4.73 |
| 16 | 100 | 2 | 40 | 148.16 ± 24.43 | 35.88 ± 5.17 | 86.01 ± 3.71 |
| 17 | 100 | 1 | 20 | 298.71 ± 17.81 | 32.27 ± 7.43 | 81 ± 4.19 |

Furthermore, the particle size of the microsphere decreased as the stirring time increased. This might be because of the higher shear forces responsible for the breakdown of the particle size.

Out of the 17 prepared formulations, Formulation 7 exhibited the lowest particle size of 84 ± 19.97 µm, while formulation two exhibited the highest particle size of 315.21 ± 13.43 µm.

### Response 2 ($R^2$): effect of the independent variable on drug loading

The $R^2$ of drug loading was 0.7846, and the adjusted $R^2$ was 0.5076, representing a well fit.

The Model F-value of 2.83 indicates that the model is significant ($p < 0.05$). In this case, A is a significant model term.

The 3D response surface plot revealing the influence of the independent variable on drug loading is shown in Figure 2. This study unfolds that, with the increase in the polymer-to-drug ratio, there was an increase in drug loading. However, the drug loading declined with the increment in the solvent ratio. With the increase in the solvent ratio, drug loading might have been decreased due to the alcohol-induced cosolvent effect (Qiao *et al*., 2018). Drug loading also decreased with the increase in stirring time. However, the effect of solvent ratio and stirring time in drug loading was not significant.

From the 17 different formulations, the lowest drug loading was observed in Formulation 7 with 22.23% ± 4.17%, while Formulation 2 presented 42% ± 7.31%.

### Response 3 ($R^3$): effect of independent variables on entrapment efficiency

The $R^2$ of drug entrapment efficiency was 0.8297, and the adjusted $R^2$ was 0.6108, representing a well fit.

The Model F-value of 3.79 implies that the model is significant ($p < 0.05$). In this case, C is a significant model term.

The 3D response surface plot unveiling the influence of an independent variable on drug entrapment efficiency is shown in Figure 3. This study suggests the increment in the drug-to-polymer ratio results in an increment in entrapment efficiency. This observation might be due to the availability of a greater amount of polymers for the complete encapsulation of the EnM molecule (Thapa *et al*., 2018). Entrapment efficiency was increased with the increase in the solvent ratio, which might be because of a decline in the alcohol concentration in higher solvent ratio, resulting in a lower alcohol-induced cosolvent effect. However, the effect of the solvent ratio on entrapment efficiency was not significant. There was a significant decline in drug entrapment efficiency with the increase in stirring time, which may be due to prolonged exposure of the microspheres under a higher shear force that is sufficient

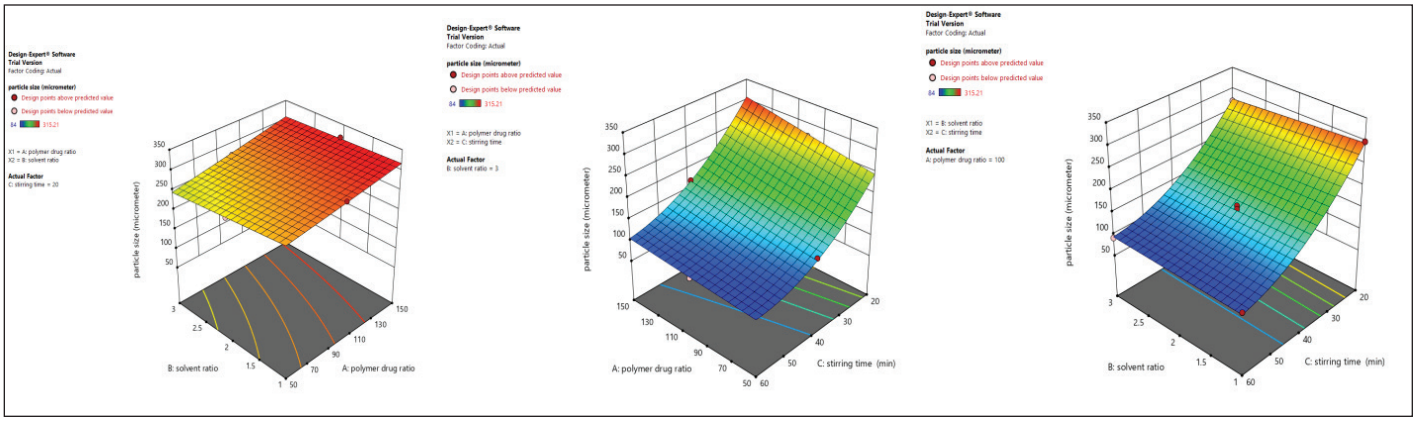


**Figure 1.** 3D response surface plot unveiling the simultaneous influence of independent variables on particle size in Formulation-A.

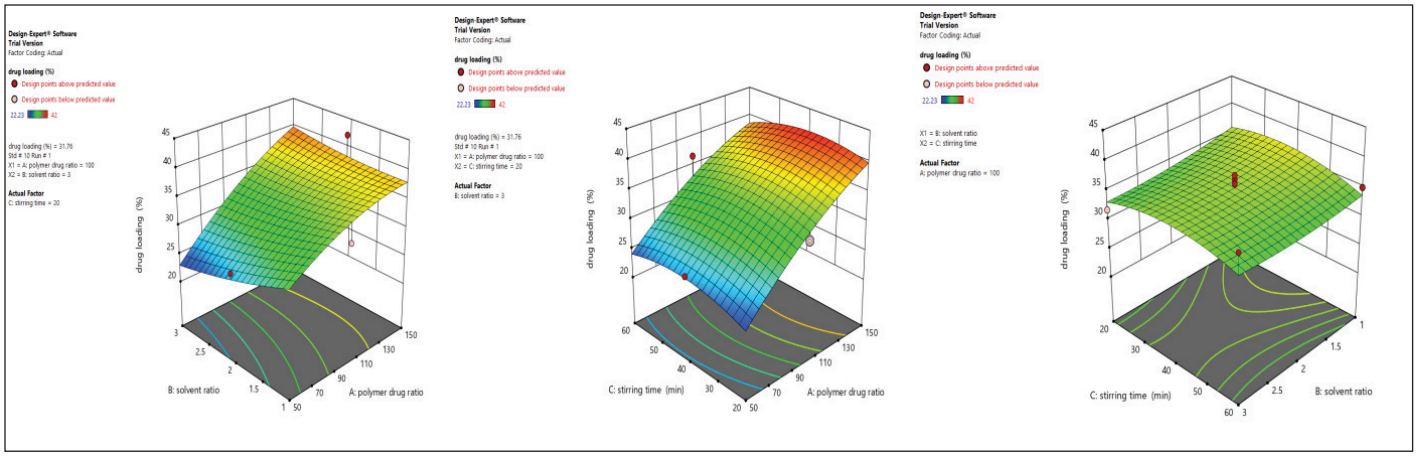


**Figure 2.** 3D response surface plot unveiling simultaneous influence of independent variables on drug loading % in Formulation-A.

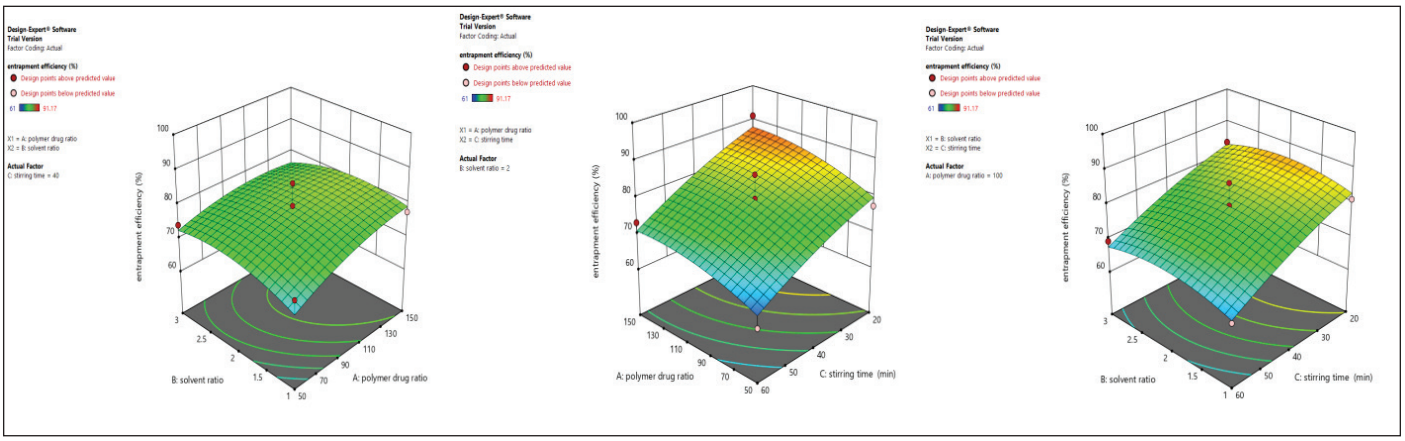


**Figure 3.** 3D response surface plot unveiling the simultaneous influence of independent variables on entrapment efficiency % in Formulation-A.

to break the microspheres resulting in a decrease in entrapment efficiency.

From the 17 formulations, the maximum % drug entrapment efficiency was observed in Formulation 2 with 91.17% ± 3.17%, and the minimum % EnM entrapment efficiency was observed in Formulation 7 with 61 ± 1.89.

### Particle size, drug loading, entrapment efficiency, and % yield of the optimized formulation

EnM-loaded optimized ethanol microsphere (Formulation-A) was selected based on minimum particle size, maximum drug loading, and entrapment efficiency. The particle size of the optimized formulation was 143.11 ± 27.75 µm, the drug loading was 37.31% ± 5.73%, and the entrapment efficiency was 76.89% ± 4.97%. The morphological shape of Formulation-A was found to be spherical and is shown in Figure 4. Similarly, the particle size, drug loading, and entrapment efficiency of Formulation-B were 158.13 ± 25.11 µm, 40.13% ± 6.12%, and 99.19% ± 1.24%, respectively. The drug encapsulation efficiency and drug loading in Formulation-A were comparatively lower than Formulation-B. It might be because of the presence of ethanol, which increases the aqueous solubility of the EnM, while in Formulation-B, drug loading and encapsulation efficiency are higher because of the absence of alcohol-induced cosolvent effect and lower solubility of EnM in acetonitrile as compared to alcohol (Qiao *et al*., 2018). The percentage yield of Formulation-A and Formulation-B was 34.19% and 29.314%, respectively.

### Buoyancy

The buoyancy percentage of Formulation-A and Formulation-B after 12 hours was found to be 67% ± 3.82% and 61% ± 2.71%, respectively. The floating ability of Formulation-A was higher, which might be due to the presence of large air-core resulting in a decrease in density of the microsphere compared to the gastric fluid (Bhardwaj *et al*., 2014).

### Micrometric study

Both formulations were better in terms of flowability. The angle of repose value for Formulation-A and Formulation-B was found to be 18 ± 2.75º and 23.2 ± 2.12º, while the Hausner's ratio value was found to be 1.19 ± 0.0002 and 1.19 ± 0.0002,

**Figure 4.** The morphological shape of floating microspheres observed through an Olympus BX53 research microscope (A). Formulation of EnM-loaded floating microspheres by solvent evaporation technique (B).

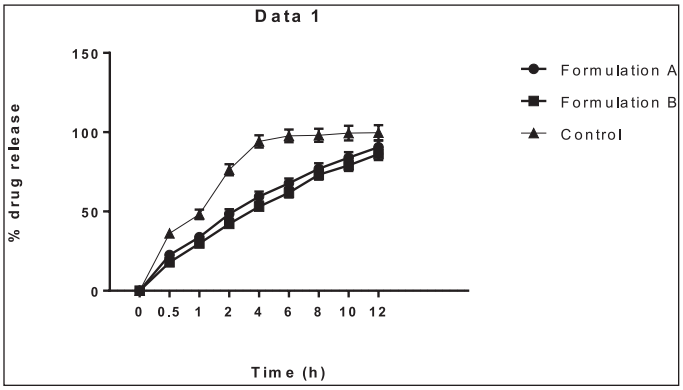


**Figure 5.** *In vitro* drug release profile of Formulation-A, Formulation-B, and control in the acidic buffer (pH 1.2).

respectively. Similarly, Carr's index value of Formulation-A and Formulation-B was found to be 16.25 ± 0.91 and 18.47 ± 1.002, respectively, indicating their excellent compressibility. Both the formulations were better in terms of flow properties with a low angle of repose, Carr's index, and low Hausner's ratio.

### *In vitro* drug release study

It was observed that the *in vitro* drug release of Formulation-A was greater than Formulation-B in the simulated gastric fluid (acidic buffer, pH 1.2) as shown in Figure 5. The cumulative percentage drug release of Formulation-A and

Formulation-B was 90.52% ± 4.11% and 86.23% ± 3.81%, respectively, as shown in Table 4. The greater cumulative drug release in Formulation-A was due to the use of the ethanol. As a solvent, ethanol might act as a cosolvent during the dissolution of the microsphere since the solubility of EnM is higher in alcohol compared to acetonitrile, consequently enhancing solubilization of EnM itself (Qiao *et al*., 2018). The *in vitro* drug release of Formulation-A was nonsignificantly higher than Formulation-B at 1 and 8 hours ($p > 0.05$). Otherwise, the *in vitro* EnM release of Formulation-A and Formulation-B was significantly higher than the control ($p < 0.05$). The polymer HPMC was used as a swelling agent and ethyl cellulose was used to increase the buoyancy of the microspheres (Kausik *et al*., 2015).

**Table 4.** Cumulative % of drug release of Formulation-A and Formulation-B with time ($n = 3$).

| Time (hour) | Cumulative % of EnM release | | Control |
|---|---|---|---|
| | Formulation-A | Formulation-B | |
| 0.5 | 22.56 ± 2.38 | 17.92 ± 1.21 | 36.17 ± 2.11 |
| 1 | 33.82 ± 2.64 | 29.77 ± 1.62 | 48.15 ± 2.98 |
| 2 | 48.38 ± 3.01 | 42.13 ± 2.01 | 76.36 ± 3.51 |
| 4 | 59.47 ± 3.22 | 53.01 ± 2.84 | 94.21 ± 3.88 |
| 6 | 67.81 ± 3.05 | 61.87 ± 3.05 | 97.64 ± 4.01 |
| 8 | 76.94 ± 3.46 | 73.14 ± 3.12 | 98.01 ± 4.22 |
| 10 | 83.99 ± 3.58 | 79.04 ± 3.47 | 99.48 ± 4.68 |
| 12 | 90.52 ± 4.11 | 86.23 ± 3.81 | 99.67 ± 4.77 |

The result of the drug release from the microsphere was fitted to the different release kinetics: "zero-order," "first-order," "Higuchi," and "Korsmeyer–Peppas model", which were taken into consideration. The *in vitro* drug release kinetics for both Formulation-A and Formulation-B in the acidic buffer (pH 1.2) is depicted in Tables 5 and 6, respectively. For Formulation-A, the maximum $R^2$ value of (0.988) in the simulated gastric fluid (pH 1.2) was observed with the "Korsmeyer–Peppas model", although the $R^2$ value of 0.988 resembles the "Higuchi model" as well. The latter was not considered because of the less number of intersecting points compared to the Korsmeyer–Peppas model. $R^2$ values for the "first-order model" and "zero-order model" were observed to be 0.986 and 0.932, respectively. The different release kinetics in the gastric fluid are shown in Figure 6. Similarly, for Formulation-B, the maximum $R^2$ value of 0.985 in the simulated gastric fluid (pH 1.2) was observed with "Higuchi model", followed by the "first-order model" ($R^2 = 0.989$), "Korsmeyer–Peppas model" ($R^2 = 0.985$), and "zero-order model" ($R^2 = 0s.956$). It was observed that Formulation-B followed "Higuchi model kinetics". The different release kinetics for Formulation-B in a gastric fluid are shown in Figure 7.

Hence, from this study, it is concluded that the EnM release from Formulation-A followed "Korsmeyer–Peppas" model kinetics. Similarly, the EnM release from Formulation-B followed the Higuchi model.

**Table 5.** *In vitro* drug release kinetics of Formulation-A in the acidic buffer (pH 1.2).

| Time (T) (minute) | Sq. root of time | LogT | % CDR of Enalapril microspheres | Fraction EnM release | Log % CDR | % EnM remaining | Log % EnM remaining |
|---|---|---|---|---|---|---|---|
| 30 | 5.47 | 1.477 | 22.56 | 0.2256 | 1.35 | 77.44 | 1.888 |
| 60 | 7.74 | 1.778 | 33.82 | 0.3382 | 1.52 | 66.18 | 1.820 |
| 120 | 10.95 | 2.079 | 48.38 | 0.4838 | 1.68 | 51.62 | 1.712 |
| 240 | 15.49 | 2.380 | 59.47 | 0.5947 | 1.77 | 40.53 | 1.607 |
| 360 | 18.97 | 2.556 | 67.81 | 0.6781 | 1.83 | 32.19 | 1.507 |
| 480 | 21.90 | 2.681 | 76.94 | 0.7694 | 1.88 | 23.06 | 1.362 |
| 600 | 24.49 | 2.778 | 83.99 | 0.8399 | 1.92 | 16.01 | 1.204 |
| 720 | 26.83 | 2.857 | 90.52 | 0.9051 | 1.95 | 9.49 | 0.977 |

**Table 6.** *In vitro* drug release kinetics of Formulation-B in the acidic buffer (pH 1.2).

| Time (T) (minute) | Sq. root of time | Log T | % CDR of Enalapril microspheres | Fraction EnM release | Log % CDR | % EnM remaining | Log % EnM remaining |
|---|---|---|---|---|---|---|---|
| 30 | 5.47 | 1.477 | 17.92 | 0.1792 | 1.25 | 82.08 | 1.91 |
| 60 | 7.74 | 1.778 | 29.77 | 0.2977 | 1.47 | 70.23 | 1.84 |
| 120 | 10.95 | 2.079 | 42.13 | 0.4213 | 1.62 | 57.87 | 1.76 |
| 240 | 15.49 | 2.380 | 53.01 | 0.5301 | 1.72 | 46.99 | 1.67 |
| 360 | 18.97 | 2.556 | 61.87 | 0.6187 | 1.79 | 38.13 | 1.58 |
| 480 | 21.90 | 2.681 | 73.14 | 0.7314 | 1.86 | 26.86 | 1.42 |
| 600 | 24.49 | 2.778 | 79.04 | 0.7904 | 1.89 | 20.96 | 1.32 |
| 720 | 26.83 | 2.857 | 86.23 | 0.8623 | 1.93 | 13.71 | 1.13 |

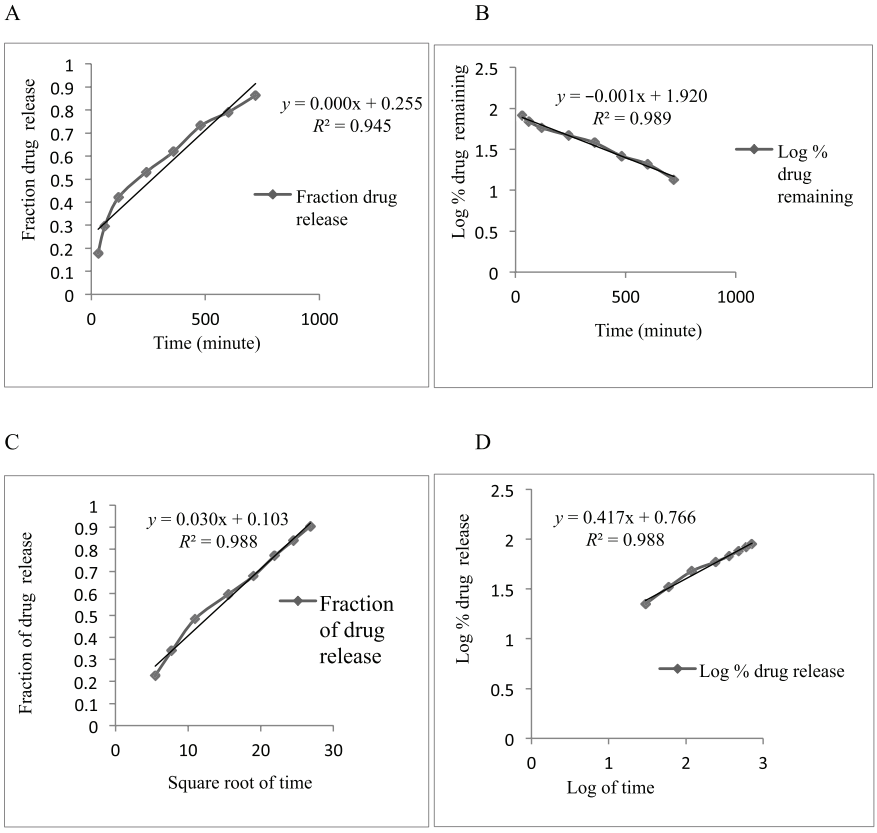


**Figure 6.** Release kinetics of Formulation-A in zero-order (A), first-order (B), Higuchi model (C), and Korsmeyer–Peppas model (D) in the acidic buffer (pH 0.1).

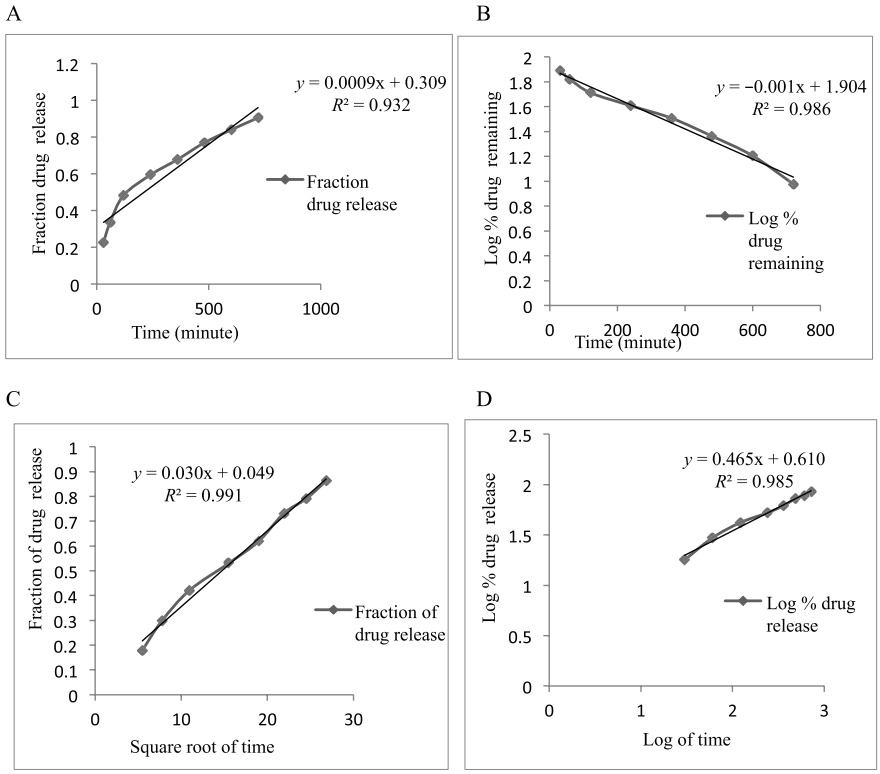


**Figure 7.** Release kinetics of Formulation-B in zero-order (A), first-order (B), Higuchi model (C), and Korsmeyer–Peppas model (D) in the acidic buffer (pH 0.1).

## CONCLUSION

EnM-loaded floating microspheres were successfully prepared by the solvent evaporation method and optimized by the response surface method. The optimized Formulation-A exhibited particle size of 143.11 ± 27.75 µm, drug loading of 37.31% ± 5.73%, and entrapment efficiency of 76.89% ± 4.97%. The *in vitro* drug release of Formulation-A was higher than that of Formulation-B. Both the formulations have shown good buoyancy for more than 12 hours with a good sustained release property.

## ACKNOWLEDGEMENTS

The authors sincerely acknowledge Lomus Pharmaceuticals (Kathmandu, Nepal) for kindly providing the gift sample of EnM. They also sincerely thank Dr. Anand Kumar for providing the laboratory facility to successfully carry out the research work.

## ETHICAL APPROVAL AND CONSENT TO PARTICIPATE

Not applicable.

## HUMAN AND ANIMAL RIGHTS

No humans/animals were considered for this study.

## CONSENT FOR PUBLICATION

Not applicable

## AVAILABILITY OF DATA AND MATERIALS

The data sets supporting the results of this research will be available from Chhitij Thapa, upon request.

## CONFLICT OF INTEREST

There are no conflicts of interest related to the publication of this paper.

## FUNDING

This study was funded by the Universal College of Medical Sciences, Siddhartha Nagar, Nepal.

## REFERENCES

Abbas Z, Marihal S. Gellan gum-based mucoadhesive microspheres of almotriptan for nasal administration: formulation optimization using factorial design, characterization and *in vitro* evaluation. J Pharm Bioallied Sci, 2014; 6(1):269.

Agrawal GR, Wakte P, Shelke S. Formulation, physicochemical characterization, and *in vitro* evaluation of human insulin-loaded microspheres as a potential oral Carrier. Prog Biomater, 2017; 6:125–36.

Amid M, Manap Y, Azmira F, Hussin M, Sarker ZI. A novel liquid/liquid extraction process composed of surfactant and acetonitrile for purification of polygalacturonase enzyme from *Durio zibethinus*. J Chromatogr B Analyt Technol Biomed Life Sci, 2015; 993:1–8.

Ammar HO, Ghorab MM, Mahmoud AA, Noshi SH. Formulation of risperidone in floating microparticles to alleviate its extrapyramidal side effects. Future J Pharm Sci, 2016; 2:43–59.

Asija R, Sharma D, Mali KR. Development and evaluation of ethyl cellulose-based floating microspheres of atorvastatin by novel solvent evaporation matrix erosion method. Pharm Chem J, 2015; 2(1):14–24.

Beringhs AOR, Fonseca ABS, Campos AMD, Sonaglio D. Association of PLGA microspheres to carrier pellets by fluid bed coating: a novel approach towards improving the flowability of microparticles. J Pharm, 2018; 2018:1–12.

Bhardwaj P, Chaurasia D, Singh R, Swarup A. Development and characterization of novel site-specific hollow floating microspheres bearing 5-Fu for stomach targeting. Sci World J, 2014; 2014:1–11.

Campbell N, Young ER, Drouin D, Legowski B, Adams MA, Farrell J, Kaczorowski J, Lewanczuk R, Lum-Kwong MM, Tobe S. A framework for discussion on how to improve prevention, management, and control of hypertension in Canada. Can J Cardiol, 2012; 28:262–9.

Chatterjee S, Salaün F, Campagne C. Development of multilayer microcapsules by a phase coacervation method based on ionic interactions for textile applications. Pharmaceutics, 2014; 6:281–97.

Farooq U, Khan S, Nawaz S, Ranjha NM, Haider MS, Khan MM, Dar E, Nawaz A. Enhanced gastric retention and drug release via the development of novel floating microspheres based on Eudragit E100 and polycaprolactone: synthesis and *in vitro* evaluation. Des Monomers Polym, 2017; 20(1):419–33.

Gao, HL, Jiang X. The progress of novel drug delivery systems. Acta Pharm Sin, 2017; 52(2):181–8.

Garg R, Gupta G. Gastro retentive floating microspheres of silymarin: preparation and *in vitro* evaluation. Trop J Pharm Res, 2010; 9(1):59–66.

Gaur PK, Mishra S, Bajpai M. Formulation-And evaluation of controlled release of telmisartan microsphere: *in vitro*/*in vivo* study. J Food Drug Anal, 2014; 22:543.

Gupta R, Prajapati SK, Pattnaik S, Bhardwaj P. Formulation and evaluation of novel stomach specific floating microspheres bearing famotidine for treatment of gastric ulcer and their radiographic study. Asian Pac J Trop Biomed, 2014; 4(9):729–35.

Hu M, Guo J, Yu Y, Cao L, Xu Y. Research advances of microencapsulation and its prospects in the petroleum industry. Materials (Basel), 2017; 10(4):369.

Ipate AM, Hamciue C, Kalvachev Y, Gherman S. New cryogels based on polymers and zeolite L for controlled Enalapril Maleate release. J Drug Deliv Sci Technol, 2018; 44:505–12.

Jagtap YM, Bhujbal RK, Ranade AN, Ranpise NS. Effect of various polymers concentrations on the physicochemical properties of floating microspheres. Indian J Pharm Sci, 2012; 74(6):512–20.

Kausik YA, Tiwari AK, Gaur A. Role of excipients and polymeric advancements in preparation of floating EnM delivery systems. Int J Pharm Investig, 2015; 5(1):01–12.

Nila MV, Sudhir MR, Cinu TA, Aleykutty NA, Jose S. Floating microspheres of carvedilol as gastroretentive drug delivery system: $3^2$ full factorial design and *in vitro* evaluation. Drug Deliv, 2014; 21(2):110–17.

Patela K, Jainb PK, Baghelb R, Tagdea P, Patila A. Preparation and *in vitro* evaluation of a micro balloon delivery system for domperidone. Pharm Lett, 2011; 3:131–41.

Prajapati CV, Patel RP, Prajapati BG. Formulation, optimization, and evaluation of sustained-release microsphere of ketoprofen. J Pharm Bioallied Sci, 2012; 4(1):101–3

Qiao B, Du C, Dong R, Jin Z, Zhang Y, Ye T, Roth M. Experiment and computation of solubility and dissolution properties for Enalapril Maleate and its intermediate in pure solvents. J Chem Eng Data, 2018; 63(12):4306–13.

Ramteke KH, Jadhav VB, Kulkarni NS, Kharat AR, Diwate SB. Preparation, evaluation, and optimization of multiparticulate system of mebendazole for colon targeted drug delivery by using natural polysaccharides. Adv Pharm Bull, 2015; 5(3):361–71.

Savjani KT, Gajjar AK, Savjani JK. Drug solubility: importance and enhancement techniques. ISRN Pharm, 2012; 2012:1–10.

Senthikumar S, Jaykar B, Kavimani S. Formulation, characterization and *in vitro* evaluation of floating microsphere containing rabeprazole sodium. Int J Ther Pharm Sci, 2010; 1(6):274–82.

Sharma M, Kohli S, Dinda A. *In-vitro* and *in-vivo* evaluation of repaglinide loaded floating microspheres prepared from different viscosity grades of HPMC polymer. Saudi Pharm J, 2015; 23:675–82.

Subham B, Gaurav C, Dilipkumar P, Gosh AK. Investigation on crosslinking density for development of novel interpenetrating polymer network (IPN) based formulation. J Sci Ind Res, 2010; 69:777–84.

Swamy BY, Prasad CV, Prabhakar MN, Rao KC, Subha MCS, Chung I. Biodegradable chitosan-g-poly(methacrylamide) microspheres for controlled release of hypertensive drug. J Polym Environ, 2013; 21:1128–34.

Tamizharasi S, Sivakumar T, Rathi JC. Preparation and evaluation of aceclofenac floating oral delivery system. Pharm Sin, 2011; 2:43–53.

Thabet Y, Walsh J, Breitkreutz J. Flexible and precise dosing of Enalapril Maleate for all pediatric age groups utilizing orodispersible minitablets. Int J Pharm, 2018; 541:136–42.

Thapa C, Ahad A, Aqil M, Imam SS, Sultana Y. Formulation and optimization of nanostructured lipid carriers to enhance the oral bioavailability of telmisartan using Box–Behnken design. J Drug Deliv Sci Technol, 2018; 44:431–9.

Vaidya A, Pathak RP, Pandey MR. Prevalence of hypertension in the nepalese community triples in a year: a repeat cross-sectional study in rural Kathmandu. Indian Heart J, 2012; 6402:128–31.

Wang W, Zhang J, Yang S, Zhang H, Yang H, Yue G. Experimental study on the angle of repose of pulverized coal. Particuology, 2010; 8(5):482–6.

Wen H, Jung H, Li X. Drug delivery approaches in addressing clinical pharmacology- related issues: opportunities and challenges. AAPS J, 2015; 17(6):1327–40.

Zhang W, Chen L, Zhe A, Liu G, Zhang L, Wang Y, Shao Y, Liu Y. Gastro retentive floating microspheres of carvedilol: preparation, *in vitro*, and *in vivo* characterization. J Biomater Tissue Eng, 2016; 6:74–8.

**How to cite this article:**
Kumal VB, Thapa C, Ghimire P, Chaudhari P, Yadhav J. Formulation and optimization of Enalapril Maleate loaded floating microsphere using Box–Behnken design: *in vitro* study. J Appl Pharm Sci, 2020; 10(08):095–104.